

Calorimetric and transport investigations of $\text{CePd}_{2+x}\text{Ge}_{2-x}$ ($x=0$ and 0.02) up to 22 GPa

H. Wilhelm

*Département de Physique de la Matière Condensée, Université de Genève, Quai Ernest-Ansermet 24, 1211 Geneva 4, Switzerland
and Max-Planck Institute for Chemical Physics of Solids, Nöthnitzer Strasse 40, 01187 Dresden, Germany*

D. Jaccard

Département de Physique de la Matière Condensée, Université de Genève, Quai Ernest-Ansermet 24, 1211 Geneva 4, Switzerland

(Received 24 April 2002; published 29 August 2002)

The influence of pressure on the magnetically ordered $\text{CePd}_{2.02}\text{Ge}_{1.98}$ has been investigated by a combined measurement of electrical resistivity $\rho(T)$ and ac calorimetry $C(T)$, for temperatures in the range $0.3 \text{ K} < T < 10 \text{ K}$ and pressures p up to 22 GPa. Simultaneously, CePd_2Ge_2 has been examined by $\rho(T)$ down to 40 mK. In $\text{CePd}_{2.02}\text{Ge}_{1.98}$ and CePd_2Ge_2 the magnetic order is suppressed at a critical pressure $p_c = 11.0 \text{ GPa}$ and $p_c = 13.8 \text{ GPa}$, respectively. In the case of $\text{CePd}_{2.02}\text{Ge}_{1.98}$ the temperature coefficient A of $\rho(T)$ not only indicates the loss of magnetic order but also the ac signal $1/V_{ac} \propto C/T$ recorded at low temperature. The residual resistivity is extremely pressure sensitive and passes through a maximum and then a minimum in the vicinity of p_c . The (T, p) phase diagram and the $A(p)$ dependence of both compounds can be qualitatively understood in terms of a pressure-tuned competition between magnetic order and the Kondo effect according to the Doniach picture. The temperature-volume (T, V) phase diagram of CePd_2Ge_2 combined with that of CePd_2Si_2 shows that in stoichiometric compounds mainly the change of interatomic distances influences the exchange interaction. It will be argued that in contrast to this the much lower p_c value of $\text{CePd}_{2.02}\text{Ge}_{1.98}$ is caused by an enhanced hybridization between $4f$ and conduction electrons.

DOI: 10.1103/PhysRevB.66.064428

PACS number(s): 62.50.+p, 75.30.Mb, 75.40.Cx, 72.15.Cz

I. INTRODUCTION

The application of external pressure on metals with strong correlations is an established technique to tune their ground-state properties. The electronic interactions in heavy-Fermion (HF) compounds can be influenced in such a way that high pressure favors the Kondo interaction in Ce compounds¹⁻⁹ and the Ruderman-Kittel-Kasuya-Yoshida (RKKY) interaction in Yb systems.^{10,11} Thus, pressure suppresses (favors) long-range magnetic order and enhances (weakens) the screening of the localized $4f$ electrons. If both interactions are of similar strength in the vicinity of a critical pressure p_c , often a deviation from the Fermi-liquid (FL) behavior is observed and some Ce compounds even attain a superconducting ground state.

Electrical resistivity measurements as a function of temperature, $\rho(T)$, are the standard method to explore the low-temperature phase diagram of HF systems up to pressures $p \approx 20 \text{ GPa}$. It is desirable to measure thermodynamic quantities, notably the specific heat $C(T)$ in these extreme conditions. The accessible pressure range for specific-heat experiments was limited to 2–3 GPa since adiabatic techniques demand large sample masses and thus, a large cell volume. For an anvil type of high pressure cell a much smaller sample volume is required, which makes an adiabatic measurement a hopeless venture. Among the nonadiabatic (or dynamic) methods, ac calorimetry^{12,13} is a suitable technique to be used at high pressures. Very high sensitivity can be achieved, whereas the absolute accuracy is less than for adiabatic techniques.

A major step towards measuring $C(T)$ under extreme conditions has been achieved by implementing the ac technique in a Bridgman type of pressure cell suited for 10

GPa.¹⁴ The sample was embedded in a soft mineral (steatite) and an ac current was supplied to a heater close to the sample. The experimental findings have been confirmed by an independent study using a diamond-anvil cell with He as pressure-transmitting medium and laser heating.^{7,15} Motivated by these results we assembled the ac calorimetry in a Bridgman type of high-pressure cell capable of reaching 25 GPa and temperatures of the order of 30 mK.¹⁶

So far, only CeCu_2Ge_2 and CeRu_2Ge_2 , where Ge is an isoelectronic substitute for Si, have been studied extensively under pressure. The former compound exhibits a phase diagram similar to that of CeCu_2Si_2 but shifted by 9.4 GPa.¹⁷ Close to the critical pressure, the long-range magnetic order is suppressed and superconductivity appears like that in CeCu_2Si_2 at low pressure.¹⁸ The temperature-volume (T, V) phase diagram of CeRu_2Ge_2 is identical to that of the solid-solution $\text{CeRu}_2(\text{Si}_{1-x}\text{Ge}_x)_2$.⁶ In contrast to CeCu_2Ge_2 no superconductivity is observed around the magnetic/nonmagnetic borderline as in CeRu_2Si_2 at ambient pressure. These observations support the notion that the Ge substitution mainly has the effect of reducing the hybridization between the $4f$ and conduction electrons due to the expansion of the unit cell volume. This argument does not seem to be limited to compounds crystallizing in the ThCr_2Si_2 type of structure. Another example is the magnetically ordered CeCu_5Au that can be pressure tuned into a nonmagnetic ground state, analogous to the HF prototype CeCu_6 at ambient pressure.¹⁹ The pressure study revealed a deviation from FL behavior and a low-temperature anomaly in $\rho(T)$ close to p_c , which could be interpreted as faint traces of a superconducting state.⁸

All these studies have in common that pressure has been applied to stoichiometric compounds. Small deviations from stoichiometry are believed to result in strong effects on the

electronic correlations. Detailed investigations of the influence of Ni excess in $\text{Ce}_{1.005}\text{Ni}_{2+z}\text{Ge}_{2-z}$ have shown that a low residual resistivity ρ_0 is a crucial requirement for the occurrence of incipient superconductivity at ambient pressure²⁰ and that the transition temperature can be shifted upwards by carefully adjusting the Ni excess.²¹ For the stoichiometric sample, however, pressure had to be applied to achieve superconductivity.²² The combination of these results have led to the hypothesis that an enhanced hybridization due to an electronically different environment of the Ce ions is a crucial ingredient to reduce p_c and to achieve a superconducting ground state.

In this paper we report on results of $\rho(T)$ experiments on CePd_2Ge_2 as well as ac calorimetry and $\rho(T)$ measurements on $\text{CePd}_{2.02}\text{Ge}_{1.98}$ performed in *one* pressure experiment. CePd_2Ge_2 enters an antiferromagnetically ordered phase at $T_N \approx 5.1$ K.^{23–26} Its Si counterpart, the HF system CePd_2Si_2 exhibits a similar magnetic structure with $T_N \approx 10$ K.^{27,28} Several groups have confirmed the occurrence of a superconducting ground state if the magnetic order is suppressed by external pressure ($p_c = 2.8$ GPa).^{3–5,29–32} If the change of interatomic distances is the main source of altering the exchange coupling between $4f$ and conduction electrons, J , then CePd_2Ge_2 should reveal a pronounced variation of $T_N(p)$. The interest in high-pressure studies on $\text{CePd}_{2.02}\text{Ge}_{1.98}$ is to explore the role of stoichiometry on J and thus on p_c . Measuring simultaneously $C(T)$ and $\rho(T)$ has the advantage that independent information about the strength of electronic correlations from the *same* specimen can be obtained.

In order to draw a credible conclusion about the pressure response of both compounds, it is essential to expose both samples to the *same* pressure conditions. The best way to achieve this is to place both specimens adjacent to each other in the *same* pressure cell.

II. EXPERIMENTAL DETAILS

A. Sample preparation and characterization

The $\text{CePd}_{2+x}\text{Ge}_{2-x}$ compounds have been prepared by melting Ce (4N), Pd (5N), and Ge (6N) according to the composition in an arc ($x=0$) or an induction furnace ($x=0.02$) under Ar (6N) atmosphere. The samples have been melted several times to achieve good homogeneity. Mass loss during melting and annealing ($\text{CePd}_{2.02}\text{Ge}_{1.98}$ at 1420 K and CePd_2Ge_2 at 1470 K for 2 days) was negligible. A part of the polycrystalline ingots has been analyzed by x-ray powder diffraction. The diffraction pattern contained only peaks according to the ThCr_2Si_2 structure ($I4/mmm$). The magnetic structure of CePd_2Ge_2 consists of ferromagnetic planes stacked antiferromagnetically along the [110] direction with moments ($\mu = 0.85\mu_B$ at 1.8 K) parallel to the stacking direction.^{23,33,34} No information about the magnetic structure of $\text{CePd}_{2.02}\text{Ge}_{1.98}$ is available, but it is very likely that the small Pd excess does not change the antiferromagnetic structure.

The measurements of the specific heat, dc magnetic susceptibility, and electrical resistivity at ambient pressure re-

TABLE I. Ambient pressure data of $\text{CePd}_{2.02}\text{Ge}_{1.98}$ and CePd_2Ge_2 . The Néel temperature T_N is the mean value of specific heat, dc magnetic susceptibility, and electrical resistivity measurements. The specific heat can be described by $C = \gamma T + \beta T^3 \exp(-\Delta/T)$ for $T \leq 2$ K. μ_{eff} is the effective magnetic moment, Θ the Curie-Weiss temperature, ρ_0 the residual resistivity, and RRR the ratio $\rho(295 \text{ K})/\rho_0$.

	$\text{CePd}_{2.02}\text{Ge}_{1.98}$	CePd_2Ge_2
a (Å)	4.3399(7)	4.3411(5)
c (Å)	10.0343(19)	10.0417(5)
V (Å ³)	189.00(7)	189.23(5)
T_N (K)	5.16(8)	5.12(7)
γ [mJ/(mol K ²)]	101(5)	44(1)
β [mJ/(mol K ⁴)]	148(5)	234(6)
Δ (K)	0.8(1)	1.6(1)
μ_{eff} (μ_B) at 300 K	2.1	2.5
Θ (K)	-24(5)	-16(3)
ρ_0 ($\mu\Omega$ cm)	1.4(1)	1.7(1)
RRR	32(3)	29(3)

vealed for both compounds a phase transition into an antiferromagnetically ordered phase at about 5.1 K (Table I). The low-temperature specific heat ($0.3 \text{ K} < T \leq 2 \text{ K}$) can be described by the sum of an electronic (γT) and a magnonlike T^3 part with a gap Δ in the excitation spectrum. The increased γ value of the Pd-rich compound with respect to the stoichiometric one points to the enhanced correlations. The γ and Δ values of CePd_2Ge_2 obtained here are larger than those reported in Ref. 26 due to the enlarged temperature range accessible in the present study. However, the absolute values of C_p at T_N are almost the same. The entropy release at T_N is $S/R \approx 0.8 \ln 2$ and reaches $\ln 2$ at about 9 K for both compounds. The high-temperature magnetic susceptibility can be described by a Curie-Weiss law $\chi \propto \mu_{\text{eff}}^2 / (T - \Theta)$, with an effective moment μ_{eff} close to the free moment value and Θ the Curie-Weiss temperature. The residual scattering is rather low in both compounds; the nonstoichiometric sample has the lower ρ_0 value.

B. High-pressure setup

Samples with cross sections of $23 \times 59 \mu\text{m}^2$ ($x=0$) and $22 \times 48 \mu\text{m}^2$ ($x=0.02$) have been cut from the polycrystalline ingots and placed into the pressure chamber (internal diameter of 1 mm).¹⁶ A small piece of Pb served as pressure gauge³⁵ and was connected in series to the samples for four-point measurements. The samples have been arranged in the pressure chamber in such a way that the crystallographic c axis was parallel to the pressurizing force. For the ac calorimetry measurements, the sample itself was used as heater and was thermally excited by an oscillating heating power $P = P_0 [1 + \cos(\omega t)]$ due to an applied ac voltage of frequency $\omega/2$. At steady state it increases the sample temperature by ΔT above the bath temperature T_0 . This temperature increase contains a time-independent offset $T_{\text{dc}} = P_0/\Lambda$, with Λ being the thermal conduction of the heat link between sample and pressure cell (to a first approxima-

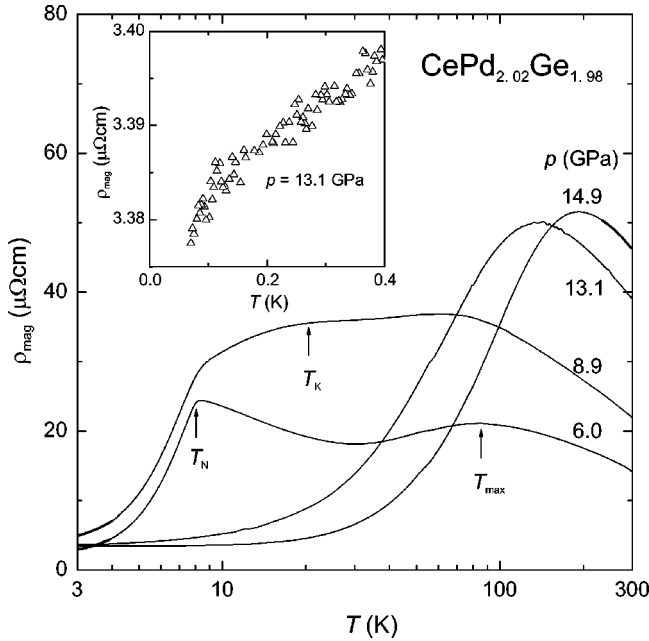


FIG. 1. The magnetic part $\rho_{\text{mag}}(T)$ of the electrical resistivity of $\text{CePd}_{2.02}\text{Ge}_{1.98}$ vs temperature T in a semilogarithmic plot. The antiferromagnetic transition produces a cusp at T_N . The scattering of carriers at the ground state and excited crystal-field levels produce two maxima at T_K and T_{max} . Inset shows that an additional phase transition at high pressure might be responsible for the decrease of $\rho_{\text{mag}}(T)$ at about 110 mK.

tion: the pressure-transmitting medium, i.e., steatite). In ideal conditions the oscillatory part of ΔT is $T_{\text{ac}} = P_0 / (\omega C_p)$.¹² These temperature oscillations have been measured with a AuFe/Au thermocouple attached to the sample. The thermovoltage V_{ac} arises from the temperature difference between the sample (at $T_0 + \Delta T$) and the edge of the sample chamber (at T_0).¹⁶

The dynamic response of the sample involves two time constants $\tau_1 = C_p / \Lambda$ and τ_2 . The former expresses the thermal coupling between the sample and the temperature bath, whereas the latter represents a characteristic time for the sample to reach thermal equilibrium. When the measuring frequency fulfills the condition $\omega \tau_1 > 1 \gg \omega \tau_2$, the ac technique yields the specific heat of the sample. In the course of the experiment, this condition was checked at several temperatures and pressures. The frequencies used were in the range $750 \text{ Hz} \leq \omega \leq 3000 \text{ Hz}$. The condition $\omega \tau_2 \ll 1$ is fulfilled for metals because they ensure high thermal conductivity within the sample.

The inverse of the recorded lock-in voltage V_{ac} is proportional to C/T , since the temperature dependence of the absolute thermoelectrical power, $S(T) \propto T$, is a fairly good assumption at $T < 1 \text{ K}$. Above this temperature the $S(T)$ dependence is certainly different and $1/V_{\text{ac}}$ has to be interpreted with caution. Nevertheless, the present setup has several advantages. First, it is possible to check whether a pronounced anomaly in $1/V_{\text{ac}}$ is related to the sample or not with an independent $\rho(T)$ measurement on the *same* sample. Second, it excludes an additional source of pressure inhomoge-

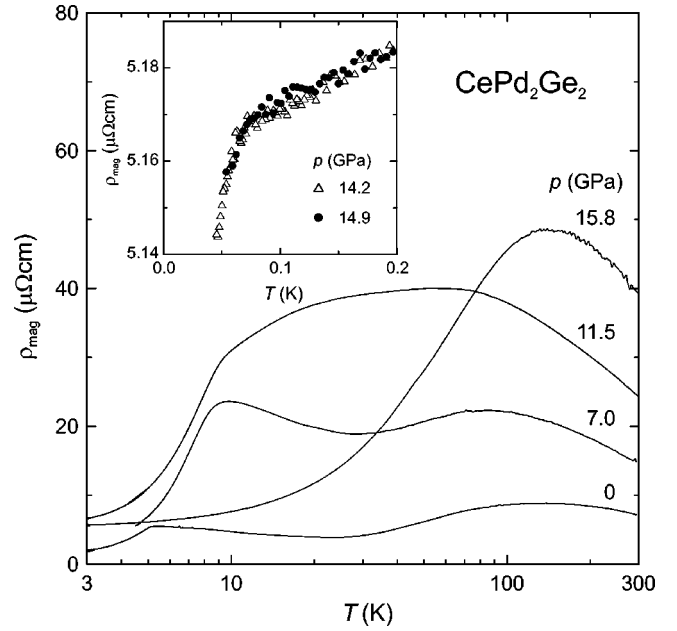


FIG. 2. Temperature dependence of the magnetic part of the electrical resistivity $\rho_{\text{mag}}(T)$ of CePd_2Ge_2 in a semilogarithmic plot. The similarity of the high-pressure curves to those of $\text{CePd}_{2.02}\text{Ge}_{1.98}$ (cf. Fig. 1) is evident. The small drop in $\rho_{\text{mag}}(T)$ at 70 mK above 14 GPa (inset) might indicate an additional phase transition.

neity due to a heater attached to the sample. Third, internal temperature gradients can be reduced as much as possible.

With such an arrangement it is, in principle, possible to calibrate the AuFe/Au thermocouple up to very high pressures and over a wide temperature range.³⁶ Here, we have only determined $S(T)$ at 4.2 K and 1.0 K to get a rough estimate of the influence of pressure on $S(T)$.³⁷ The obtained values of the absolute thermopower of AuFe at 4.2 K and 1.0 K at 12 GPa are about 20% smaller than the values at ambient pressure. These rather small changes show that the interpretation of the results reported in this work is not affected qualitatively if the ambient pressure values of $S(T)$ are used.

The sample chamber has been carefully reexamined after pressure release to rule out changes in the positions of the voltage leads connected to the samples. The overall shape of the pressure cell as well as its initial diameter were almost unchanged and the distance between the voltage leads increased by less than 5%. Taking this uncertainty in the geometrical factor as well as the change in volume at high pressure into account, the absolute value of $\rho(T)$ can be determined within 20%.

III. RESULTS

A. Transport measurements

The entrance into the magnetically ordered state is clearly visible by a cusp in $\rho_{\text{mag}}(T)$ of $\text{CePd}_{2.02}\text{Ge}_{1.98}$ and CePd_2Ge_2 (Figs. 1 and 2). The magnetic contribution $\rho_{\text{mag}}(T)$ to $\rho(T)$ has been obtained by subtracting a phononic contribution, approximated as $\rho_{\text{ph}}(T) = 0.1 \mu\Omega \text{ cm/K} \times T$, from the raw data. Qualitatively, both compounds show the same pressure

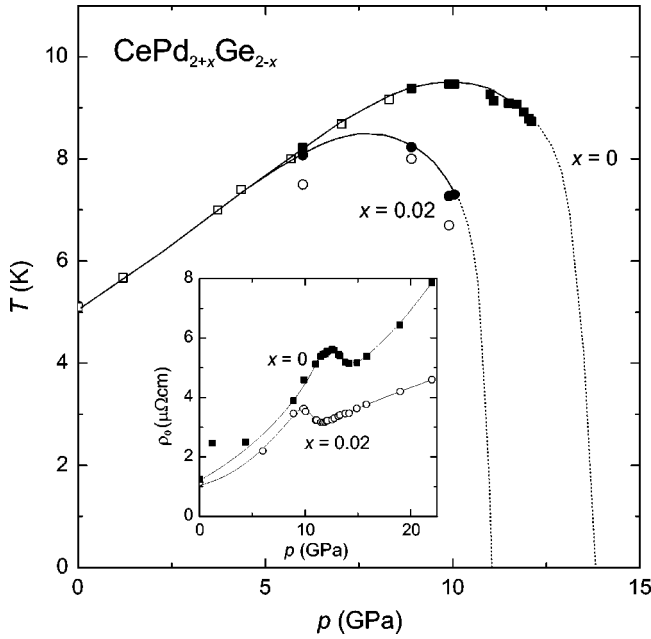


FIG. 3. Pressure dependence of T_N for $\text{CePd}_{2+x}\text{Ge}_{2-x}$ ($x=0$ and 0.02). The extrapolation $T_N \rightarrow 0$ assumes critical pressures $p_c = 11.0$ GPa ($x=0.02$) and 13.8 GPa ($x=0$). Two data sets of $T_N(p)$ for $x=0$ obtained for different samples match perfectly. The T_N values for $x=0.02$ obtained by the ac calorimetry are represented by open circles. Inset shows that a pronounced variation of the residual resistivity ρ_0 with pressure is observed in both compounds.

dependence: Pressure shifts T_N upwards, the signature of the phase transition broadens, and within a small pressure range, the traces of the phase transition vanish. $\rho_{\text{mag}}(T)$ exhibits two maxima, reflecting the Kondo scattering from the ground state and excited crystal-field levels as often observed for other compounds (indicated by T_K and T_{max} , respectively, in Fig. 1).^{8,16} Furthermore, a small and reproducible decrease in $\rho_{\text{mag}}(T)$ has been detected at very low temperature (insets of Figs. 1 and 2). It occurs in a narrow pressure range in the apparently nonmagnetic phase below 110 mK for $\text{CePd}_{2.02}\text{Ge}_{1.98}$ whereas it was found in CePd_2Ge_2 at somewhat lower temperature (70 mK). In each case an increased measuring current density suppressed the anomaly.

These measurements reveal the pressure dependence of T_N , as depicted in Fig. 3. As a criterion for T_N , the intersection of two tangents drawn to $\rho(T)$ has been used. In the case of CePd_2Ge_2 both data sets obtained for different samples from the same batch in different pressure cells match perfectly (open and filled squares in Fig. 3). The initial pressure shift $\partial T_N / \partial p = 0.51(1)$ K/GPa is slightly higher than that reported in Ref. 38. The same value is obtained for $\text{CePd}_{2.02}\text{Ge}_{1.98}$ if the values of T_N at ambient pressure and 6 GPa are used. At higher pressures, however, both $T_N(p)$ variations are clearly different. In $\text{CePd}_{2.02}\text{Ge}_{1.98}$, T_N does not reach the same absolute value as in the stoichiometric compound and the magnetic order vanishes already at $p_c = 11.0$ GPa, compared to $p_c = 13.8$ GPa for CePd_2Ge_2 . Thus, the Pd excess has led to a reduction of p_c by 2.8 GPa.

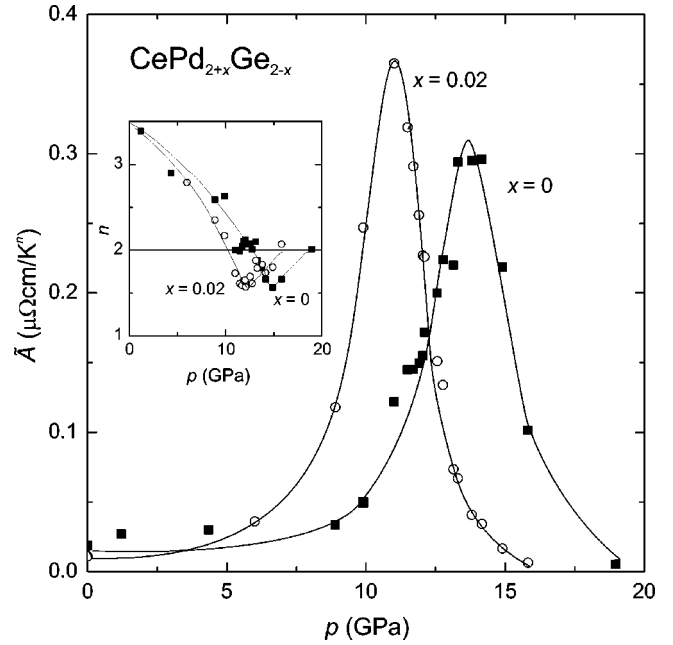


FIG. 4. Temperature coefficient \tilde{A} obtained from a fit, $\rho_{\text{mag}}(T) = \rho_0 + \tilde{A}T^n$, to the data of $\text{CePd}_{2+x}\text{Ge}_{2-x}$ ($x=0$ and 0.02) below 2 K vs pressure p . \tilde{A} peaks at 11.0 GPa and 13.8 GPa for $x=0.02$ and $x=0$, respectively. Inset shows the exponent n used to describe $\rho_{\text{mag}}(T)$ at different pressures.

The extrapolation $T_N \rightarrow 0$ (dotted lines in Fig. 3) is based on the assumption that the maximum in the $\tilde{A}(p)$ dependence can be taken as critical pressure. The \tilde{A} values have been obtained from fits of $\rho_{\text{mag}}(T) = \rho_0 + \tilde{A}T^n$ to the data below 2 K, with \tilde{A} and n as fitting parameters. The lower bound to the fit is given by the accessible temperature and is about 40 mK. The value for the upper limit is a compromise between an as narrow as possible temperature interval and the reliability of the deduced parameters. The pressure dependence of the temperature coefficient \tilde{A} is qualitatively similar for both compounds and shows a pronounced anomaly that is assumed to be the hallmark of the magnetic/nonmagnetic phase transition (see Fig. 4). Both $\tilde{A}(p)$ variations can be mapped on top of each other if a pressure shift of $\Delta p_{\text{max}(\tilde{A})} = 2.8$ GPa is taken into account. In the magnetically ordered phase the exponent $n > 2$, whereas $n = 2$ is found in the Fermi-liquid regime far above p_c (inset of Fig. 4). Exponents smaller than 2 are observed in a certain pressure range around p_c . A minimum $n \approx 1.6$ is attained just above p_c for both compounds. Within a small pressure range around p_c , $\rho_{\text{mag}}(T)$ cannot be described by a quadratic temperature dependence even if the temperature interval is $40 \text{ mK} < T < 0.6$ K. Similar observations have been reported for CePd_2Si_2 (Refs. 29 and 32) and other systems, such as CeRu_2Ge_2 (Refs. 6) and CeCu_5Au .⁸

Approaching the verge of magnetism seems also to affect the residual resistivity ρ_0 . It is very sensitive to small pressure changes and exhibits anomalies around p_c , which are qualitatively the same for both compounds (see inset of Fig. 3). Just below p_c , ρ_0 attains a local maximum and passes

TABLE II. Pressure values where the residual resistivity ρ_0 and the fitting parameter of $\rho_{\text{mag}}(T)$ as well as $1/V_{\text{ac}}$ for $T \rightarrow 0$ show anomalies. At p_c^{cal} the calculated unit cell volume of CePd_2Ge_2 is equal to that of CePd_2Si_2 at its critical pressure ($p_c = 3.9$ GPa.³²) Each anomaly occurring in $\text{CePd}_{2.02}\text{Ge}_{1.98}$ is also seen in CePd_2Ge_2 , but shifted by Δp as indicated in the last column.

Pressure (GPa)	$\text{CePd}_{2.02}\text{Ge}_{1.98}$	CePd_2Ge_2	Δp (GPa)
$p_{\text{max}\{\rho_0\}}$	9.7	12.3	2.6
$p_c = p_{\text{max}\{\tilde{A}\}}$	11.0	13.8	2.8
$p_{\text{min}\{\rho_0\}}$	11.6	14.5	2.9
$p_{\text{max}\{1/V_{\text{ac}}\}_{T \rightarrow 0}}$	11.7		
$p_{\text{min}\{n\}}$	12.1	14.6	2.5
p_c^{cal}	14.2	14.4	0.2

through a local minimum above p_c . Upon further pressure increase ρ_0 continuously increases, and at 22 GPa it reaches several times its ambient pressure value. This variation reflects intrinsic effects since a change of the geometrical factor in such a peculiar manner can be ruled out.

The comparison of the resistivity data presented above reveals that pressure has qualitatively the same effect on both compounds. The main difference is that for $\text{CePd}_{2.02}\text{Ge}_{1.98}$ less pressure [$\Delta p = 2.7(2)$ GPa] is required to achieve the same effect, as in CePd_2Ge_2 . Table II summarizes several quantities that show pronounced anomalies in their pressure behavior. From this we infer that not only interatomic distances are important for J since the difference in unit cell volume at ambient pressure cannot explain such a large shift in p_c .

B. ac calorimetry on $\text{CePd}_{2.02}\text{Ge}_{1.98}$

Figure 5 shows the inverse of the registered lock-in signal V_{ac} below 10 K at various pressures. The pronounced anomaly in $1/V_{\text{ac}}(T)$ for pressures between 6.0 GPa and 10 GPa is caused by the entrance into the antiferromagnetically ordered phase. Taking the temperature of the maximum as T_N yields lower T_N values, like those shown in Fig. 3. T_N taken from the midpoint of the $1/V_{\text{ac}}$ anomaly at 6 GPa is the same as that deduced from $\rho(T)$. At higher pressure, however, this definition yields T_N values greater than those obtained from $\rho(T)$. The height of the anomaly decreases and it becomes a very broad feature as the system approaches p_c . A similar broadening upon approaching p_c has been reported for CeRu_2Ge_2 (Ref. 7) and CePd_2Si_2 (Ref. 29) examined in pressure cells with solid He as pressure-transmitting medium, despite their lower p_c values.

From a general point of view, this might be due to inhomogeneous pressure conditions that are always present regardless the pressure medium and the absolute value of p_c . Close to p_c the $T_N(p)$ variation is very strong and a small pressure gradient can easily generate $\Delta T_N \approx 1$ K. However, other intrinsic effects cannot be excluded to be responsible for a broadening in the vicinity of p_c .

A very interesting observation is the pressure dependence of the value of $1/V_{\text{ac}}$ taken at the lowest temperature reached in each pressure run (inset of Fig. 5). Upon approaching p_c it

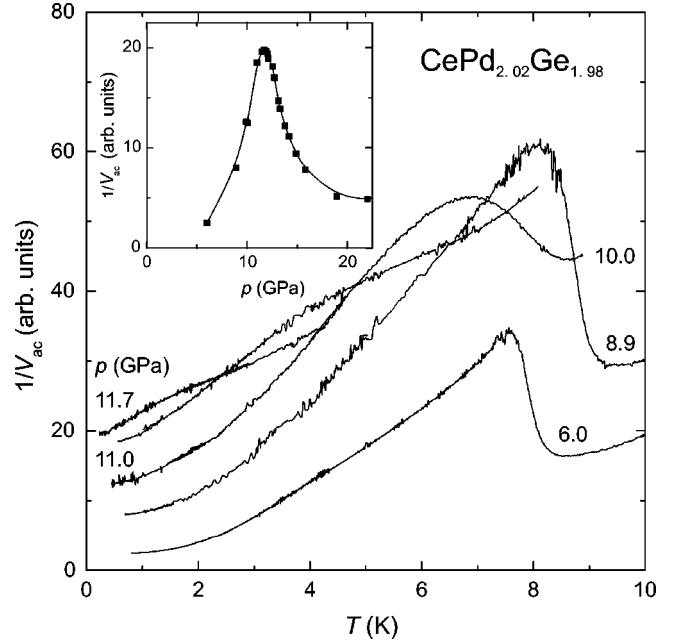


FIG. 5. Temperature dependence of the inverse lock-in voltage V_{ac} of $\text{CePd}_{2.02}\text{Ge}_{1.98}$. The entrance into the antiferromagnetically ordered state is clearly visible. Inset shows that the values of $1/V_{\text{ac}} \propto C/T$ taken at low temperature show a pronounced peak in the vicinity of p_c .

strongly increases, reaches a maximum just above p_c [which was inferred from the $\tilde{A}(p)$ anomaly], and levels off at high pressure. As was pointed out above, $1/V_{\text{ac}}(T) \propto C/T$ at low temperature can be regarded as a direct measure of the electronic correlations. The pronounced pressure dependence of $1/V_{\text{ac}}$ shows that the electronic correlations are considerably enhanced as pressure approaches p_c and that the signal originates mainly from the sample.

IV. DISCUSSION

In the following, we will first compare the $T_N(V)$ dependence of CePd_2Ge_2 with that of CePd_2Si_2 . Thereafter, an elaborate discussion of the pressure effects on the $\text{CePd}_{2+x}\text{Ge}_{2-x}$ compounds ($x=0$ and 0.02) will reveal a possible explanation of the observed similarities as well as the differences.

The (T, p) phase diagram of each $\text{CePd}_{2+x}\text{Ge}_{2-x}$ compound ($x=0$ and 0.02) presented in Fig. 3 can be qualitatively understood within the Doniach picture.³⁹ Pressure tunes the characteristic energy scales, $T_K \propto \exp[-1/Jn(E_F)]$ and $T_{\text{RKKY}} \propto [Jn(E_F)]^2$, involved in the Kondo effect and the RKKY interaction, respectively. Here J is the exchange coupling between $4f$ and conduction electrons and $n(E_F)$ is the density of states at the Fermi energy E_F . The RKKY interaction dominates the Kondo effect for small $Jn(E_F)$ values as in CePd_2Ge_2 at low pressures where T_K is very small. The slight difference in composition has little effect on T_N at ambient pressure and on its pressure dependence below 6 GPa. In both samples, $Jn(E_F)$ is enhanced by pressure and forces the system into a nonmagnetic state for $p > p_c$.

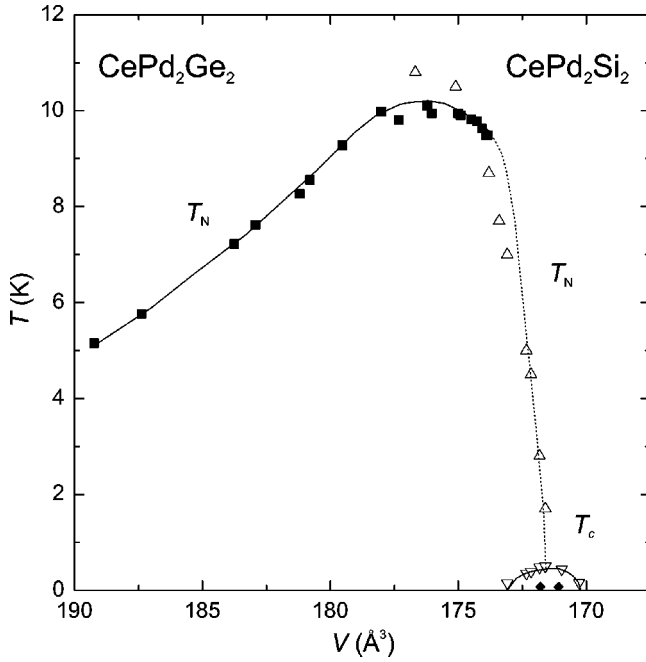


FIG. 6. Transition temperatures of CePd_2Ge_2 and CePd_2Si_2 as a function of a calculated unit cell volume, V . T_N and T_c represent the Néel temperature and the superconducting transition temperature, respectively. The data of CePd_2Si_2 (open symbols) are taken from Ref. 32. The temperature derivative of $\rho_{\text{mag}}(T)$ was used as T_N criterion.

If the unit cell volume is the crucial parameter that determines T_N , then it should be possible to plot the $T_N(p)$ data of CePd_2Ge_2 and its Si counterpart CePd_2Si_2 in a common (T, V) phase diagram. As pressure has tuned the unit cell volume of CePd_2Ge_2 to that of CePd_2Si_2 , both T_N values should be comparable, as the $T_N(V)$ variation of the solid-solution $\text{CePd}_2(\text{Si}_{1-x}\text{Ge}_x)_2$ suggest.⁴⁰ The transformation of pressure into volume was done with a bulk modulus $B_0 = 120$ GPa (and $B' = 4$ for its pressure dependence) for both compounds. This is a reasonable assumption for ternary Ce compounds, crystallizing in the ThCr_2Si_2 type of structure, as was pointed out in Ref. 6. We used as a unit cell volume of CePd_2Si_2 at ambient pressure, $V_0 = 176.83 \text{ \AA}^3$, which is the mean value of the literature data.^{5,28,33,41,42} Figure 6 exhibits a pronounced $T_N(V)$ variation, starting at $T_N = 5.1$ K, passing through a maximum of about 10 K, and eventually approaching zero. The extrapolation $T_N \rightarrow 0$ yields $V = 171.51 \text{ \AA}^3$, which corresponds to a pressure of 14.4 GPa, very close to $p_c = 13.8$ GPa deduced from the maximum in $\tilde{A}(p)$. CePd_2Si_2 reaches this volume at $p_c = 3.9$ GPa. This p_c value agrees perfectly with that found in a thorough investigation of the strain enhancement of superconductivity.³²

The almost perfect match of the two data sets emphasizes the importance of the sample orientation with respect to the direction of the applied force. Figure 6 shows only data from samples with their crystallographic c axis parallel to the applied force exerted to the anvils. The additional uniaxial strain component along the c axis strongly affects the anisotropy of the tetragonal ThCr_2Si_2 structure. It is known from x-ray absorption studies⁴³ that a change of the c -axis lattice

parameter results in a varying chemical bonding strength between the Ce ions and their ligands. A change in the Ce valence, however, is thought to influence only the a -axis lattice parameter, and vice versa. Thus, it seems that the additional uniaxial stress is necessary to change the hybridization in an effective way. In CePd_2Si_2 , it shifts p_c from 2.8 GPa to 3.9 GPa and leads to an increase in the superconducting transition temperature of about 40% (Ref. 32) compared to values obtained from samples in a configuration where the crystallographic c axis was perpendicular to the external force.^{3,4,29,30}

The combined phase diagram clearly demonstrates the analogy between CePd_2Ge_2 at high pressure and CePd_2Si_2 at moderate pressures. It can provide an idea about the sudden decrease of $\rho_{\text{mag}}(T)$ in $\text{CePd}_{2.02}\text{Ge}_{1.98}$ and CePd_2Ge_2 at 110 mK and 70 mK, respectively (insets of Figs. 1 and 2). The reduced volume where these anomalies occur is similar to the volume where superconductivity is found in CePd_2Si_2 (Fig. 6). An interpretation as incipient superconductivity is therefore one possible explanation, especially if the reported properties of $\text{CeNi}_{2+x}\text{Ge}_{2-x}$ (Refs. 20, 21, and 44) and CePd_2Si_2 (Refs. 29, 45) are recalled. In the former system, $\rho = 0$ was only achieved after ρ_0 had been reduced below 1–2 $\mu\Omega \text{ cm}$. For those samples with higher ρ_0 values only traces of superconductivity appeared. Also for the latter compound, high-purity samples ($\rho_0 < 1 \mu\Omega \text{ cm}$) seem to be required for a complete superconducting transition.⁴

The difference in the p_c values and the $\tilde{A}(p)$ dependence of $\text{CePd}_{2.02}\text{Ge}_{1.98}$ and CePd_2Ge_2 can also be understood qualitatively within the Doniach picture. Magnetic order is a cooperative phenomenon involving the alignment of spins over distances that are large compared to the lattice parameter. It is very unlikely that a small change in the Ce-ligand configuration will influence the RKKY interaction and $J \approx J'$ seems to be justified, with J and J' being the exchange coupling for $x=0$ and $x=0.02$, respectively. The almost identical T_N values at ambient pressure corroborates this assumption. For the Kondo effect, however, only the local environment of the Ce ions is essential and therefore, a small change in its configuration sphere should influence T_K . It seems very likely that the additional Pd in $\text{CePd}_{2.02}\text{Ge}_{1.98}$ occupies Ge sites and/or interstitial sites and might influence the local environment of the Ce ions, resulting in $J' > J$. Within a certain limit this hypothesis is supported by the different γ values at ambient pressure (Table I). Furthermore, the x-ray data of $\text{CePd}_{2.02}\text{Ge}_{1.98}$ reveal that the c -axis lattice parameter is slightly lower, whereas the a -axis lattice parameter is unchanged within the standard deviation. Thus, the Pd excess could have caused a stronger hybridization between the $4f$ and conduction electrons already at ambient pressure, as was argued above. Results of a thorough investigation of the influence of the Ni excess in $\text{Ce}_{1.005}\text{Ni}_{2+z}\text{Ge}_{2-z}$ encourage this argumentation.²⁰ As a function of the Ni content, the c -axis lattice parameter and ρ_0 showed a minimum at $z = 0.02$ and a complete superconducting transition occurred close to this value at ambient pressure, whereas pressure had to be applied to achieve a superconducting ground state in the stoichiometric compound.²² With these assumptions

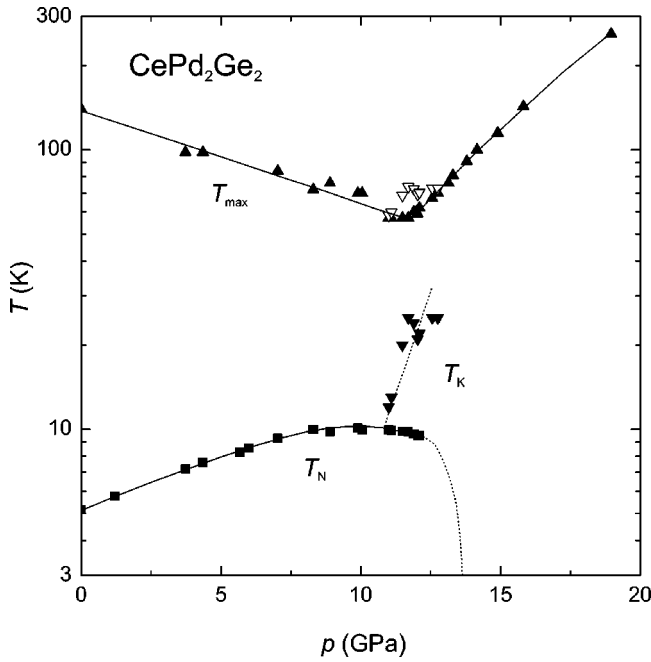


FIG. 7. Pressure dependence of some characteristic temperatures, T_{\max} , T_N , and T_K of CePd_2Ge_2 in a semilogarithmic plot. The pressure dependence of T_{\max} shows a minimum close to p_c . The open symbols represent calculated data of T_K^h (see text).

$T_{\text{RKKY}}(J)$ will be of comparable strength to $T_K(J)$ and $T_K(J')$ at a critical value $J'_c < J_c$. Therefore, p_c of $\text{CePd}_{2.02}\text{Ge}_{1.98}$, determined by J'_c , is lower than p_c of CePd_2Ge_2 , given by J_c . As a consequence of this consideration, a shifted $\tilde{A}(p)$ dependence follows, since $\tilde{A} \propto T_K^{-2}$, as is experimentally found and depicted in Fig. 4.

The Kondo temperature in CePd_2Ge_2 at low pressures is small in comparison to the crystal-field splitting $\Delta_1 = 110$ K and $\Delta_2 = 220$ K.²⁶ Therefore, $\rho_{\text{mag}}(T)$ shows only one maximum at T_{\max} at low pressure. Around p_c , however, two maxima at T_K and T_{\max} occur, reflecting the Kondo scattering from the ground state and excited state, respectively (Figs. 1 and 2). The low-temperature maximum emerges at a pressure of about 11 GPa and shifts to higher temperatures with increasing pressure, as shown in Fig. 7. This might reflect an enhanced screening of the magnetic moments by the conduction electrons and thus point to an increasing role of the Kondo effect. As a consequence, the anomaly at low temperature has to be related to T_K . Both anomalies in $\rho_{\text{mag}}(T)$ seem to merge in the vicinity of p_c , indicating the entrance into the intermediate valence regime. In this region the crystalline electrical field levels cease to exist as well-defined excitations. In the case of two excited crystal field levels, Hanazawa *et al.*⁴⁶ have introduced a second Kondo temperature T_K^h at high temperature. It is related to T_K by $T_K^h = \sqrt[3]{T_K \Delta_1 \Delta_2}$. Using the assumption that Δ_1 and Δ_2 decrease under pressure with the same rate as in CePd_2Si_2 (Ref. 33), the T_K^h values can be calculated as a function of pressure (open symbols in Fig. 7). A good agreement is achieved with the measured values of T_{\max} . Similar considerations can be made for $\text{CePd}_{2.02}\text{Ge}_{1.98}$, resulting in the

same phase diagram but shifted by 2.8 GPa to lower pressures.

The analysis of the low-temperature behavior of $\rho_{\text{mag}}(T)$ has revealed almost the same anomalies in ρ_0 , \tilde{A} , and n for $\text{CePd}_{2.02}\text{Ge}_{1.98}$ and CePd_2Ge_2 . Of particular interest is the strong pressure dependence of ρ_0 (inset of Fig. 3). It is an additional example of a pressure-dependent residual resistivity scattering in HF compounds already pointed out in Ref. 17. The anomalies in $\rho_0(p)$ cannot be caused by lattice defects and impurities alone like in conventional metals. The independent-electron approximation [$\rho_0 \propto 1/(k_F^2 l)$, with k_F being the Fermi wave number and l the mean free path] suggests that pressure should affect ρ_0 only weakly since both k_F and l react upon pressure only through a small change of electron density and interatomic distances. In metals with strongly interacting electrons and magnetic order, the contributions to ρ_0 are not well understood. So far, a noticeable $\rho_0(p)$ dependence has been found in several HF systems either in the magnetic phase [CeCu_5Au (Ref. 19) and YbCu_2Si_2 (Ref. 10)], close to p_c (CeAl_3)⁴⁷ or in the paramagnetic phase [CeCu_2Ge_2 and CeCu_2Si_2 (Ref. 17)]. Following the suggestion by Miyake and Maebashi,⁴⁸ quantum critical fluctuations should give rise to an enhanced impurity potential. It leads to an increase of ρ_0 through non-magnetic impurity scattering near a ferromagnetic or antiferromagnetic quantum critical point if many-body corrections of scattering are taken into account. This possibility and the wealth of $\rho_0(p)$ anomalies reported so far might indicate that only a part of ρ_0 is due to static disorder and that the large variation of $\rho_0(p)$ is an intrinsic property of a weakly disordered Kondo lattice.¹⁹

The deviation from FL behavior around p_c is an established fact and can be understood in the framework of spin fluctuation theory.^{49,50} For spin fluctuations with three-dimensional (3D) character, $\rho(T) = \rho_0 + \tilde{A}T^n$, with $n = 1.5$, is expected. The minimum values of n depicted in Fig. 4 are close to this value. It is considerably different from a linear temperature dependence that is expected for a distribution of Kondo temperatures.⁵¹ Therefore, Kondo disorder seems to be negligible.

The ac-calorimetry data revealed a pronounced variation of the ac signal recorded below 1 K. It was argued above that $1/V_{\text{ac}}$ can be taken as the linear coefficient of the specific heat, $C/T = \gamma$. Its pressure dependence is not strong enough to follow the $\tilde{A}(p)$ dependence according to the empirical Kadowaki-Woods relation.⁵² Especially at pressures above 15 GPa, the low-temperature value of $1/V_{\text{ac}}$ decreases less than expected from $\tilde{A}(p)$.³⁶ A possible reason for this deviation might be the unknown thermal properties of the pressure-transmitting medium (and perhaps also of the sample) at high pressure. They have changed significantly, which was only accounted for by adjusting the measuring frequency. A step towards a quantitative measure of C_p at these conditions would be to achieve a control of the supplied heating power and the thermal contact between sample and pressure-transmitting medium. Nevertheless, the strong

pressure dependence of $1/V_{ac}$ at low temperature is reminiscent to $\tilde{A}(p)$ and is a motivation for further studies.

V. CONCLUSION

We reported on the results of a combined electrical resistivity $\rho(T)$ and ac calorimetry, $C(T)$, investigation of the antiferromagnetically ordered $\text{CePd}_{2.02}\text{Ge}_{1.98}$ ($T_N=5.16$ K) and $\rho(T)$ measurements of CePd_2Ge_2 ($T_N=5.12$ K) for pressures up to 22 GPa. Both measuring techniques have been assembled in *one* Bridgman type of high-pressure cell. The particular sample arrangement guarantees similar pressure conditions essential for a comparison of the pressure-induced effects. The ac calorimetry and $\rho(T)$ data have been obtained from the *same* sample, which is important to demonstrate the feasibility of the ac technique at these extreme conditions. Both methods reveal a suppression of magnetic order at a critical pressure $p_c=11.0$ GPa and $p_c=13.8$ GPa for $\text{CePd}_{2.02}\text{Ge}_{1.98}$ and CePd_2Ge_2 , respectively. The inverse of the ac signal, $1/V_{ac} \propto C/T$, recorded at the lowest temperature exhibits an anomaly in the vicinity of p_c , reminiscent to $\tilde{A}(p)$, the temperature coefficient of $\rho(T)$. Although the pressure dependence of $1/V_{ac}$ is not strong enough to follow the entire $\tilde{A}(p)$ dependence according to the Kadowaki-Woods relation, it is evident that the ac signal mainly represents the sample properties. These observations demonstrate the sensitivity of the ac calorimetry to electronic

correlations despite the small sample mass (some μg). From the combined (T, V) phase diagram of CePd_2Ge_2 and CePd_2Si_2 it was concluded that interatomic distances play a crucial role for the hybridization between the $4f$ and conduction electrons, i.e., for the exchange coupling J , in the stoichiometric compound. In order to explain the large difference in the p_c values, it was argued that the Ce coordination sphere in $\text{CePd}_{2.02}\text{Ge}_{1.98}$ has changed due to the Pd excess with respect to CePd_2Ge_2 . This affects the Kondo temperature T_K , and therefore T_K will be comparable to the RKKY interaction at a lower critical value of J for $\text{CePd}_{2.02}\text{Ge}_{1.98}$. With this assumption, the shifted $\tilde{A}(p)$ variations have also been explained. The deviation of $\rho(T)$ from a Fermi-liquid behavior in the vicinity of p_c can be ascribed to 3D spin fluctuations. The strong variation of the residual resistivity ρ_0 with pressure around p_c might indicate that only a part of ρ_0 is due to static disorder. As a consequence, the assumption of a power law for $\rho(T)$ will be a subject of further careful investigations, especially at very low temperatures.

ACKNOWLEDGMENTS

We thank Y. Wang and A. Junod for fruitful discussions about the ac-calorimetric technique and R. Cartoni for technical support. The assistance of N. Caroca-Canales, H. Rave, and Z. Hossain at the MPI CPfS is acknowledged. We are grateful to A. Demuer for forwarding us the data of CePd_2Si_2 prior publication.

-
- ¹D. Jaccard, K. Behnia, and J. Sierro, *Phys. Lett. A* **163**, 475 (1992).
- ²R. Movshovich, T. Graf, D. Mandrus, J.D. Thompson, J.L. Smith, and Z. Fisk, *Phys. Rev. B* **53**, 8241 (1996).
- ³F.M. Grosche, S.R. Julian, N.D. Mathur, and G.G. Lonzarich, *Physica B* **223&224**, 50 (1996).
- ⁴N.D. Mathur, F.M. Grosche, S.R. Julian, I.R. Walker, D.M. Freye, R.K.W. Haselwimmer, and G.G. Lonzarich, *Nature (London)* **394**, 39 (1998).
- ⁵S. Raymond, D. Jaccard, H. Wilhelm, and R. Cerny, *Solid State Commun.* **112**, 617 (1999).
- ⁶H. Wilhelm, K. Alami-Yadri, B. Revaz, and D. Jaccard, *Phys. Rev. B* **59**, 3651 (1999).
- ⁷A. Demuer, C. Marcenat, J. Thomasson, R. Calemczuk, B. Salce, P. Lejay, D. Braithwaite, and J. Flouquet, *J. Low Temp. Phys.* **120**, 245 (2000).
- ⁸H. Wilhelm, S. Raymond, D. Jaccard, O. Stockert, and H. v. Löhneysen, in *Science and Technology of High Pressure*, edited by M. H. Manghanani, W. J. Nellis, and M. F. Nicol (Universities Press, Hyderabad, India, 2000), p. 697.
- ⁹H. Hegger, C. Petrovic, E.G. Moshopoulou, M.F. Hundley, J.L. Sarrao, Z. Fisk, and J.D. Thompson, *Phys. Rev. Lett.* **84**, 4986 (2000).
- ¹⁰K. Alami-Yadri, H. Wilhelm, and D. Jaccard, *Eur. Phys. J. B* **6**, 5 (1998).
- ¹¹G. Knebel, D. Braithwaite, G. Lapertot, P.C. Canfield, and J. Flouquet, *J. Phys.: Condens. Matter* **13**, 10 935 (2001).
- ¹²P.F. Sullivan and G. Seidel, *Phys. Rev.* **173**, 679 (1968).
- ¹³A. Eichler and W. Gey, *Rev. Sci. Instrum.* **50**, 1445 (1979).
- ¹⁴F. Bouquet, Y. Wang, H. Wilhelm, D. Jaccard, and A. Junod, *Solid State Commun.* **113**, 367 (2000).
- ¹⁵B. Salce, J. Thomasson, A. Demuer, J.J. Blanchard, J.M. Martinod, L. Devoille, and A. Guillaume, *Rev. Sci. Instrum.* **71**, 2461 (2000).
- ¹⁶D. Jaccard, E. Vargoz, K. Alami-Yadri, and H. Wilhelm, *Rev. High Pressure Sci. Technol.* **7**, 412 (1998).
- ¹⁷D. Jaccard, H. Wilhelm, K. Alami-Yadri, and E. Vargoz, *Physica B* **259-261**, 1 (1999).
- ¹⁸B. Bellarbi, A. Benoit, D. Jaccard, J.M. Mignot, and H.F. Braun, *Phys. Rev. B* **30**, 1182 (1984).
- ¹⁹H. Wilhelm, S. Raymond, D. Jaccard, O. Stockert, H.v. Löhneysen, and A. Rosch, *J. Phys.: Condens. Matter* **13**, L329 (2001).
- ²⁰F. Steglich, P. Gegenwart, C. Geibel, P. Hinze, M. Lang, C. Langhammer, G. Sparn, and O. Trovarelli, *Physica B* **280**, 349 (2000).
- ²¹D. Jaccard (unpublished).
- ²²D. Braithwaite, T. Fukuhara, A. Demuer, I. Shekin, S. Kambe, J.-P. Brison, K. Maezawa, T. Naka, and J. Flouquet, *J. Phys.: Condens. Matter* **12**, 1339 (2000).
- ²³B. Fåk, E. Ressouche, G. Knebel, J. Flouquet, and P. Lejay, *Solid State Commun.* **115**, 407 (2000).
- ²⁴T. Fukuhara, S. Akamaru, T. Kuwai, J. Sakurai, and K. Maezawa,

- J. Phys. Soc. Jpn. **67**, 1998 (1998).
- ²⁵H. Iwasaki, N. Kobayashi, and Y. Muto, *Physica B & C* **148**, 64 (1987).
- ²⁶M.J. Besnus, A. Essaihi, G. Fischer, N. Hamdaoui, and A. Meyer, *J. Magn. Magn. Mater.* **104-107**, 1387 (1992).
- ²⁷J.D. Thompson, R.D. Parks, and H. Borges, *J. Magn. Magn. Mater.* **54-57**, 377 (1986).
- ²⁸R.A. Steeman, E. Frikkee, R.B. Helmholtz, A.A. Menovsky, J. van den Berg, G.J. Nieuwenhuys, and J.A. Mydosh, *Solid State Commun.* **66**, 103 (1988).
- ²⁹A. Demuer, D. Jaccard, I. Shekin, S. Raymond, B. Salce, J. Thomasson, D. Braithwaite, and J. Flouquet, *J. Phys.: Condens. Matter* **13**, 9335 (2001).
- ³⁰I. Shekin, D. Braithwaite, J.-P. Brison, S. Raymond, D. Jaccard, and J. Flouquet, *J. Low Temp. Phys.* **122**, 591 (2001).
- ³¹S. Raymond and D. Jaccard, *Phys. Rev. B* **61**, 8679 (2000).
- ³²A. Demuer, A.T. Holmes, and D. Jaccard, *J. Phys.: Condens. Matter* **14**, L529 (2002).
- ³³N.H. van Dijk, B. Fåk, T. Charvolin, P. Lejay, and J.M. Mignot, *Phys. Rev. B* **61**, 8922 (2000).
- ³⁴R. Feyerherm, B. Becker, M.F. Collins, J.A. Mydosh, G.J. Nieuwenhuys, and S. Ramakrishnan, *Physica B* **241-243**, 643 (1998).
- ³⁵B. Bireckhoven and J. Wittig, *J. Phys. E* **21**, 841 (1988).
- ³⁶H. Wilhelm and D. Jaccard (unpublished).
- ³⁷We have neglected the absolute thermopower of the pure Au wire which has been annealed (3 h at 1073 K) in air in order to oxidize uncontrolled Fe impurities.
- ³⁸G. Oomi, Y. Uwatoko, E.V. Sampathkumaran, and M. Ishikawa, *Physica B* **223&224**, 307 (1996).
- ³⁹S. Doniach, *Physica B & C* **91**, 231 (1977).
- ⁴⁰I. Das and E.V. Sampathkumaran, *Phys. Rev. B* **44**, 9711 (1991).
- ⁴¹D. Rossi, R. Marazza, and R. Ferro, *J. Less-Common Met.* **66**, 17 (1979).
- ⁴²P. Link, D. Jaccard, and P. Lejay, *Physica B* **223&224**, 303 (1996).
- ⁴³E.V. Sampathkumaran, G. Kalkowski, C. Laubschat, G. Kaindl, M. Domke, G. Schmiester, and G. Wortmann, *J. Magn. Magn. Mater.* **47&48**, 212 (1985).
- ⁴⁴F.M. Grosche, P. Agarwal, S.R. Julian, N.J. Wilson, R.K.W. Haselwimmer, S.J.S. Lister, N.D. Mathur, F.V. Carter, S.S. Saxena, and G.G. Lonzarich, *J. Phys.: Condens. Matter* **12**, L533 (2000).
- ⁴⁵F.M. Grosche, I.R. Walker, S.R. Julian, N.D. Mathur, D.M. Freye, M.J. Steiner, and G.G. Lonzarich, *J. Phys.: Condens. Matter* **13**, 2845 (2001).
- ⁴⁶K. Hanazawa, K. Yamada, and K. Yoshida, *J. Magn. Magn. Mater.* **47&48**, 357 (1985).
- ⁴⁷D. Jaccard and J. Sierro, *Physica B* **206-207**, 625 (1995).
- ⁴⁸K. Miyake and H. Maebashi, *J. Phys.: Condens. Matter* **62**, 53 (2001).
- ⁴⁹A.J. Millis, *Phys. Rev. B* **48**, 7183 (1993).
- ⁵⁰T. Moriya and T. Takimoto, *J. Phys. Soc. Jpn.* **64**, 960 (1995).
- ⁵¹O.O. Bernal, D.E. MacLaughlin, H.G. Lukefahr, and B. Andraka, *Phys. Rev. Lett.* **75**, 2023 (1995).
- ⁵²K. Kadowaki and S.B. Woods, *Solid State Commun.* **58**, 507 (1986).